

Differential inhibition of water and ion channel activities of mammalian Aquaporin-1 by two structurally related bacopaside compounds derived from the medicinal plant *Bacopa monnieri*.

Jinxin V Pei, Mohamad Kourghi, Michael L De Ieso, Ewan M Campbell, Hilary S
Dorward, Jennifer E. Hardingham and Andrea J Yool

School of Medicine, University of Adelaide; Adelaide SA 5005 Australia (JVP, MK, MLDI,
JEH, AJY)

Institute for Photonics and Advanced Sensing, University of Adelaide; Adelaide SA 5005
Australia (JVP, AJY)

School of Biological Sciences, University of Aberdeen; Aberdeen AB242TZ Scotland (EMC)

Molecular Oncology Laboratory, Basil Hetzel Institute, The Queen Elizabeth Hospital,
Woodville, SA, 5011 Australia. (HSD, JEH)

Running title page:

Inhibition of aquaporin-1 by bacopasides

Corresponding author:

Prof Andrea J Yool

Medical School South level 4, Frome Rd

Adelaide SA 5005 AUSTRALIA

ph: +61 8 8313 3359

email: andrea.yool@adelaide.edu.au

fax: +61 8 8313 5384

Number of text pages: 35

Number of tables: 1

Number of figures: 7

Supplemental data files: 2

Number of words:

abstract 225

introduction 728

discussion 1500

Non-standard abbreviations: AQP (aquaporin); AqBxxx (numbered series of aquaporin modulators derived from bumetanide); AqFxxx (numbered series of aquaporin modulators derived from furosemide); methanol extract of whole *Bacopa* (meWB)

Abstract

Aquaporin-1 (AQP1) is a major intrinsic protein that facilitates flux of water and other small solutes across cell membranes. In addition to its function as a water channel in maintaining fluid homeostasis, AQP1 also acts as a non-selective cation channel gated by cGMP, a property shown previously to facilitate rapid cell migration in a AQP1-expressing colon cancer cell line. Here we report two new modulators of AQP1 channels, bacopaside I and bacopaside II, isolated from the medicinal plant *Bacopa monnieri*. Screening was conducted in the *Xenopus* oocyte expression system, using quantitative swelling and two-electrode voltage clamp techniques. Results showed bacopaside I blocked both the water (IC_{50} 117 μ M) and ion channel activities of AQP1 but did not alter AQP4 activity, whereas bacopaside II selectively blocked the AQP1 water channel (IC_{50} 18 μ M) without impairing the ionic conductance. These results fit with predictions from in silico molecular modeling. Both bacopasides were tested in migration assays using HT29 and SW480 colon cancer cell lines, with high and low levels of AQP1 expression respectively. Bacopaside I (IC_{50} 48 μ M) and bacopaside II (IC_{50} 14 μ M) impaired migration of HT29 cells, but had minimal effect on SW480 cell migration. Results here are the first to identify differential AQP1 modulators isolated from a medicinal plant. Bacopasides could serve as novel lead compounds for pharmaceutical development of selective aquaporin modulators.

Introduction

Aquaporin (AQP) water channels are in the family of major intrinsic proteins found from bacteria to humans (Agre et al., 1993; Calamita et al., 1995; Reizer et al., 1993), and are targets for the discovery of selective pharmacological modulators. Classes of aquaporins transport water and small uncharged molecules such as glycerol and urea through individual pores located in each subunit (Fu et al., 2000; Tajkhorshid et al., 2002).

An expanding role for aquaporins as multifunctional channels is being recognized (Yool and Campbell, 2012). In addition to facilitating water flux through intrasubunit pores, AQP1 also functions as a non-selective monovalent cation channel using the central pore at the four-fold axis of symmetry (Campbell et al., 2012; Yool and Weinstein, 2002; Yu et al., 2006). The ion channel conductance is activated by interaction of cGMP in the intracellular Loop D domain, and modulated by the carboxyl terminal domain (Anthony et al., 2000; Boassa and Yool, 2003; Saparov et al., 2001; Zhang et al., 2007). cGMP appears to trigger opening of cytoplasmic hydrophobic barriers in the central pore, allowing hydration and cation permeation (Yu et al., 2006). Inhibition of the AQP1 ion channel has been shown to slow cell migration rates in a colon cancer cell line that expresses high levels of AQP1 (Kourghi et al., 2016).

Defining pharmacological modulators of aquaporins has been an area of keen interest (Devuyst and Yool, 2010; Papadopoulos and Verkman, 2008; Seeliger et al., 2013). Early work identified blockers such as mercury (Preston et al., 1993), silver and gold (Niemietz and Tyerman, 2002), acetazolamide (Gao et al., 2006), and tetraethylammonium ion (Brooks et al., 2000; Detmers et al., 2006; Yool et al., 2002), but these remained limited in usefulness because of toxicity, lack of specificity, or variable efficacy across experimental systems (Yang et al., 2006; Yool, 2007). More recently, small molecule pharmacological agents with therapeutic potential have been identified. Complexes of gold-based compounds have promise for the selective block of specific classes of aquaporins; functionalized bipyrene and

terpyridines coordinating Au(III) were shown to block aquaglyceroporin AQP3 with little effect on AQP1 (Martins et al., 2013). Intracellular arylsulfonamide modulators of AQP1 include the bumetanide derivative, AqB013, which blocks AQP1 and AQP4 water permeability (Migliati et al., 2009); AqB011 which blocks the AQP1 cation channel (Kourghi et al., 2016); and the furosemide derivative AqF026 which potentiates water channel activity of AQP1 (Yool et al., 2013). Other arylsulfonamide agents have been proposed as blockers of AQP4 (Huber et al., 2009; Huber et al., 2007). , Growing evidence is demonstrating that specific arylsulfonamides act as AQP modulators in vitro and in vivo (Pei et al., 2016). Diverse small molecules acting at the extracellular side present a valuable array of novel inhibitors of AQP1 (Seeliger et al., 2013), indicating that other compounds in addition to coordinated metal ligands and arylsulfonamides are of interest for the development of AQP modulators. Lack of effect for a broad panel of AQP modulators tested in one study might reflect problems with synthesis or solubilization of the agents, or could indicate that the type of bioassay used influences apparent drug efficacy (Esteve-Font et al., 2016).

The present study was aimed at broadening the panel of AQP modulatory agents by evaluating natural medicinal plants as sources of active compounds. Quantitative swelling assays of mammalian AQP1 and AQP4 channels in the *Xenopus* expression system were used for screening extracts from a variety of traditional medicinal herbs, and identified *Bacopa monnieri* as one of several promising sources. Work here tested the hypothesis that chemical constituents of *B. monnieri* could be identified and characterized as pharmacological agents that modulate mammalian AQP1 by interacting at domains associated with pore functions.

Data here show that bacopaside I blocks both the water and ion channel activities of AQP1 but does not alter AQP4 activity, and bacopaside II selectively blocks the AQP1 water channel without impairing the ionic conductance. Results fit well with in silico docking for predicted energies of interaction at a pore-occluding intracellular site. Bacopasides I and II showed the same order of efficacy in blocking migration of AQP1-expressing HT29 colon

cancer cells, with minimal effects on SW480 cells that express AQP1 at low levels. Results here are the first to identify AQP1 channels as one of the candidate targets of action of the Ayurvedic medicinal plant, water hyssop, and to define new lead compounds for the development of AQP modulators.

Materials and Methods

Bacopa methanol extraction and fractionation

Bacopa monnieri stems and leaves were obtained with permission from The Botanic Gardens of Adelaide (Adelaide, South Australia). Chopped bacopa plant material (100 g) was dried, then refluxed in 500ml of methanol for 2 hours at room temperature. The suspension was filtered using Whatman No. 1 paper to obtain a methanol extract of whole bacopa (meWB). Half of the meWB extract was aliquoted into microfuge tubes, dried under vacuum (SpeedVac) into a solid brown paste, and reconstituted in saline for oocyte swelling assays. The other half of the meWB was fractionated using small-scale reverse phase C18 silica column (Alltech Prevail C18, Grace; Deerfield, IL). The mobile phases used for fractionation were a series of six water-methanol mixtures with H₂O:CH₃OH ratios ranging from 5:0 to 0:5. The fractions were dried in under vacuum and reconstituted in saline for oocyte swelling assays. Fractions containing AQP1 blocking activity were analyzed with mass spectrometry by Flinders Analytical (Flinders University, South Australia). Bacopaside I was identified by precise molecular weight as a major component in the active fractions, and bacopasides I and II were purchased from a commercial source (Chromadex; Irvine CA USA), solubilized in methanol to yield 100x stock solutions, and stored at -20°C. Experimental solutions were prepared by mixing the bacopaside stocks (1 part in 100) with isotonic saline or culture medium to yield final concentrations of 10 to 200 µM. Vehicle control salines were made using the same volume of methanol alone in isotonic saline or culture medium.

Oocyte preparation and cRNA injection

Unfertilized oocytes were isolated from *Xenopus laevis* frogs in accord with University Animal Ethics Committee-approved protocols, defolliculated by treatment with collagenase (type 1A, 2 mg/ml; Sigma, St. Louis, MO) and trypsin inhibitor (0.67 mg/ml; Sigma, St. Louis, MO) in OR-2 saline (82 mM NaCl, 2.5 mM KCl, 1 mM MgCl₂, and 5 mM HEPES; pH 7.6) at 16°C for

1.5 hours, washed in OR-2 saline, and then incubated in isotonic oocyte saline [96 mM NaCl, 2 mM KCl, 0.6 mM CaCl₂, 5 mM MgCl₂, and 5 mM HEPES supplemented with 10% horse serum (Sigma, St. Louis, MO), 100 U/ml penicillin, 100 µg/ml streptomycin and 50 µg/ml tetracycline, pH 7.6] at 16°C. Oocytes were injected with 1-4 ng of AQP1, AQP4 or AQP1 R159A+R160A cRNA in 50 nl sterile water and incubated for 2 to 3 days at 16-18°C to allow protein expression. Oocytes not injected with cRNA served as non-AQP-expressing control cells.

Human AQP1 (National Center for Biotechnology Information NCBI GenBank: BC022486.1) and rat AQP4 (AF144082.1) cDNAs from P. Agre (The Johns Hopkins University, Baltimore, MD) were subcloned into a modified *Xenopus* β-globin expression plasmid. The double mutant construct human AQP1 R159A+R160A cDNA was generated by site-direct mutation (QuikChange; Stratagene, La Jolla, CA) and sequenced to confirm no errors were introduced (Yu et al., 2006). cDNAs were linearized with BamHI and transcribed using T3 polymerase (T3 mMessage mMachine; Ambion Inc., Austin, TX). cRNAs were resuspended in sterile water and stored at -80°C.

Quantitative oocyte swelling assays

Immediately prior to swelling assays, control and AQP-expressing oocytes were preincubated in isotonic saline (serum- and antibiotic-free) with or without meWB or bacopaside compounds or with methanol vehicle at 16-18°C, for incubation periods as indicated. Osmotic water permeability was determined as the linear rate of change in volume as a function of time, immediately after introduction into 50% hypotonic saline (isotonic saline diluted with equal volume of water). Oocytes were imaged using a computer controlled charge-coupled-device grayscale camera (Cohu, San Diego, CA) mounted on a dissecting microscope (Olympus SZ-PT; NSW Australia). Images were taken at 0.5 frames per second for 60 seconds; cross-sectional areas were quantified using ImageJ software (Research Services Branch; National Institutes of Health, MD USA). Swelling rates were calculated as

the slopes of linear regression fits of volume as a function of time in hypotonic saline. Data were analyzed and compiled for multiple batches of oocytes for statistical analyses and to generate dose-response curves, which were fit by sigmoidal non-linear variable-slope dose-response regression functions using Prism (GraphPad Software Inc., San Diego, CA USA).

Molecular docking

In silico modeling was done with methods reported previously (Yool et al., 2013). The protein crystal structures for human AQP1 (PDB ID. 1FQY) and human AQP4 (PDB ID. 3GDB) were obtained from the protein data bank (NCBI Structure). Bacopaside I and II structures were obtained from PubChem (NCBI) and converted into a software-compatible 3D structures in .pdb format using the Online SMILES Translator and Structure File Generator (National Cancer Institute, US Dept Health and Human Services). Ligand and receptor coordinates were prepared for docking using Autodock (Version 4.2, Scripps Research Institute, La Jolla, CA USA). Autodock Vina (Trott and Olson, 2010) was used to run the flexible ligand docking simulations with two docking grids covering both intracellular and extracellular faces of the monomeric pores. 3D docking result files and docking energy values were exported from Autodock, and results were viewed using PyMol software (Version 1.8, Schrödinger, LLC). Data for AQP1 and AQP4 docking results in .pdb format are provided as Data Supplement files.

Electrophysiology

For two-electrode voltage clamp, capillary glass electrodes (1–3 MΩ) were filled with 1 M KCl. Recordings were done in standard isotonic Na⁺ bath saline containing 100 mM NaCl, 2 mM KCl, 4.5 mM MgCl₂, and 5 mM HEPES, pH 7.3. cGMP was applied extracellularly at a final concentration of 10-20 μM using the membrane-permeable cGMP analog [Rp]-8-[para-chlorophenylthio]-cGMP (Sigma Chemical, Castle Hill NSW Australia). Ionic conductance was monitored for at least 20 min after cGMP addition to allow development of maximal plateau responses. Conductance was determined by linear fit of the current amplitude as a

function of voltage, with a step protocol from +60 to -110mV and holding potential of -40 mV. After the first activation by cGMP, oocytes were incubated in isotonic saline with or without bacopaside I or bacopaside II for two hours to allow recovery. After incubation, a second application of cGMP was used to test for reactivation, to determine if any block of the ionic conductance was evident. Using the same protocol, AQP1-expressing oocytes were demonstrated previously to show cGMP-dependent activation, complete recovery during a 2 h incubation in saline alone, and full reactivation of the ionic conductance response to a second application of cGMP, whereas non-AQP1-expressing control oocytes showed a low ionic conductance and no significant response to drug treatments throughout the same protocol (Kourghi et al., 2016). Recordings were made with a GeneClamp amplifier and pClamp 9.0 software (Molecular Devices, Sunnyvale CA USA).

Cancer cell culture and migration assays

HT29 and SW480 colon cancer cell lines (from American Type Culture Collection ATCC, Manassas, VA USA) were cultured in complete medium composed of Dulbecco's Modified Eagles Medium (DMEM) supplemented with 1 x glutaMAX™ (Life Technologies Mulgrave, VIC, Australia), penicillin and streptomycin (100 U/ml each) and 10% fetal bovine serum (FBS). Cultures were maintained in 5% CO₂ at 37°C. Cells were seeded in a flat-bottom 96-well plates at 1.25 x 10⁶ cells/ml to produce a confluent monolayer. For 12 to 18 hours prior to wounding, cells were serum-starved in 2% FBS, in the presence of 400 nM of the mitotic inhibitor 5-fluoro-2'-deoxyuridine, FUDR (Parsels et al., 2004). For wounding, a sterile p10 pipette tip was attached to the end of a vacuum tube, and a circular wound was created by brief perpendicular contact of the tip with base of the well. Each well was then washed three times with phosphate buffered saline (PBS) to remove detached cell debris. Cultures were maintained during the wound closure assay in 2% FBS medium with FUDR. Wound images were imaged at 10x magnification with a Canon EOS 6D camera mounted on a Olympus inverted microscope. Image dimensions and pixel density were standardized across each image series using XnConvert software. Linear outlines and areas of the wound were

generated using ImageJ software (National Institutes of Health). Wound closure data as a function of time were calculated as a percentage of the initial wound areas for the same wells.

Quantitative RT-PCR

Cells at 70-80% confluence were harvested and RNA extracted using the PureLink™ RNA Mini kit (Life Technologies). RNA was quantified using the NanoDrop 2000 spectrophotometer (Thermo Scientific, Waltham, MA, USA) and the integrity (RIN score) assessed using the 2100 Bioanalyzer (Agilent Technologies, Santa Clara, CA, USA). RNA (500 ng) was reverse transcribed using the iScript™ cDNA synthesis kit (Bio-rad, Carlsbad, CA, USA). qPCR of AQP1 and the reference gene phosphomannose mutase 1 (PMM1) was performed using multiplex Taqman expression assays (Life Technologies) and SsoFast™ probes supermix (Bio-rad) in triplicate in the Rotorgene 6000 (Qiagen).

Western blot

Cultured cells were lysed with RIPA buffer containing 1% β -mercaptoethanol, 1% HALT protease inhibitor 100X solution, 150 U Benzonase (all from Sigma, St Louis, MO, USA) on ice for 10 minutes, homogenized by passing through a 21 gauge syringe and centrifuged 14,000 x g for 15 minutes at 4°C to pellet the cell debris. Protein was quantified (EZQ® assay, Life Technologies). Each sample (50 μ g) was resolved by SDS-PAGE on a 12% Mini-PROTEAN® TGX Stain-Free™ Gels (Bio Rad) and transferred to PVDF membranes using the Trans-Blot® Turbo™ Transfer Pack and System (Bio Rad). Membranes were blocked with TBST containing 5% skim milk for 1 hour and incubated overnight at 4°C with anti- AQP1 (H-55) (1/500; Santa Cruz, USA). Following three washes in TBST, membranes were incubated with goat anti-rabbit IgG HRP secondary antibody (1/ 2000) and Streptactin-HRP Conjugate (1/10000) (both Bio-Rad) at room temperature for 1h, and washed. Chemiluminescence using Clarity™ Western ECL Blotting Substrate (Bio-Rad) was used for detection and blots imaged using the ChemiDoc™ Touch Imaging System (Bio-Rad). Image

Lab™ Software was used to validate western blotting data via total protein normalization (Bio-Rad).

Immunocytochemistry

HT29 and SW480 cells grown on coverslips to 50% confluence were fixed with 4% paraformaldehyde and permeabilized with 0.5% Triton X-100. Image-iT® FX Signal Enhancer (Life Technologies) was used as per manufacturer's instructions. AQP1 was labelled with a 1/400 dilution of rabbit polyclonal anti-human AQP1 (Abcam®, Cambridge, UK), visualized with a secondary antibody at 1/200 dilution (goat anti rabbit IgG H&L Alexa Fluor® 568; Life Technologies). Cells were counterstained with NucBlue® Fixed Cell Ready Probes™ Reagent (Life Technologies). Coverslips were mounted in ProLong® Gold antifade reagent (Life Technologies) and imaged with a Zeiss LSM 700 microscope (Carl Zeiss, Jena, Germany).

Live cell imaging

Cells were seeded on an 8-well uncoated Ibidi µ-Slide (Ibidi, Munich Germany) at a density of 1.0×10^6 cells/ml. For 12 to 18 hours prior to wounding, cells were serum-starved in medium with 2% FBS in the presence of FUDR (400 nM). Five circular wounds were created in each well using techniques described for the migration assays (above). The slide was mounted on a Nikon Ti E Live Cell Microscope (Nikon, Tokyo Japan) in an enclosed chamber kept at 37 °C with 5% CO₂. Images were taken at 5 min intervals for 24 hours, using Nikon NIS-Elements software (Nikon, Japan). AVI files were exported from NIS-Elements and converted into TIFF files using ImageJ (NIH). Converted files were analyzed using Fiji software (Schindelin et al., 2012) with the Manual Tracking plug-in.

Cytotoxicity assay

HT29 cell viability was quantified using the AlamarBlue assay (Molecular Probes, Eugene, OR USA). Cells were plated at 10^4 cells/well in 96-well plates, and fluorescence signal levels were measured with a FLUOstar Optima microplate reader after 24 h incubation with

concentrations of bacopaside I from 0 to 100 μ M or bacopaside II from 0 to 30 μ M, to obtain quantitative measures of cell viability. Mercuric chloride (100 μ M) was used as a positive control for cytotoxicity.

Results

Extracted compounds from Bacopa monnieri inhibited AQP1 water channel activity.

Methanol-extracted whole Bacopa (meWB) reconstituted in isotonic saline ("water hyssop extract") inhibited the water permeability of AQP1-expressing oocytes (Fig 1A). After 2 hours preincubation in 1 mg/ml meWB, swelling rates of AQP1-expressing oocytes were significantly reduced ($p < 0.001$) as compared with untreated AQP1-expressing oocytes. Fractionated samples of meWB reconstituted at 0.1 mg/ml each were tested for biological activity using oocyte swelling assays (Fig 1B) after 2 hours preincubation. AQP1-mediated swelling was significantly decreased by fractions 3 and 4; other fractions had no effect. Combined fractions 3 and 4 were analyzed by mass spectrometry and revealed the presence of a major compound identified by precise molecular weight as bacopaside I. Commercially purchased bacopasides I and II were found to block osmotic water permeability in AQP1-expressing oocytes (Fig 1C) and showed a dose-dependent effect (Fig 1D). The inhibition of AQP1-mediated osmotic water fluxes showed IC_{50} values of approximately 18 μ M for bacopaside II, and approximately 117 μ M for bacopaside I. Chemical structures are shown in Fig 1E.

Inhibition by bacopasides I and II was time-dependent and reversible. AQP4-expressing oocytes showed no block of water channel activity after 2 h preincubation in isotonic saline containing bacopaside I at 178 μ M (Fig 2A). The blocking effect of bacopaside was specific for AQP1. The inhibitory effect of bacopasides I and II on AQP1 water channel activity took time to develop, with near maximum block achieved by approximately 2 h (Fig 2B). The magnitude of inhibition of AQP water flux increased as a function of the duration of preincubation in 178 μ M bacopaside I or 35 μ M bacopaside II. For bacopaside I, half-maximal block was reached after approximately 50 min, and maximum block after 120 min of preincubation. For bacopaside II, half-maximal block was reached after approximately 30 min, and maximum block after 80 min of preincubation. Longer times provided no appreciable further enhancement of the magnitude of inhibition. Comparably slow time-dependent onset

of block has been noted previously for other AQP1 ligands such as AqB013, AqB011 and AqF026, which are thought to bind at the intracellular side of the channel (Kourghi et al., 2016; Migliati et al., 2009; Yool et al., 2013), and require time to travel across the plasma membrane to the cytoplasmic side.

The blocking effects of bacopasides I and II on AQP1 water channel activity were reversible (Fig 2C). AQP1-expressing oocytes were preincubated 2 hours with 178 μ M bacopaside I or 35 μ M bacopaside II, followed by washout of the drug with isotonic saline. The osmotic water permeability showed approximately 25% recovery by 120 min after the washout of bacopaside I, and half-maximal recovery by 160 min. For bacopaside II, water permeability showed 25% recovery by 150 min after washout of the blocker, and half-maximal recovery by 200 min.

The ion channel conductance of AQP1 was inhibited by bacopaside I but not by bacopaside II. Two-electrode voltage clamp recordings from AQP1-expressing oocytes demonstrated the cGMP-dependent activation of the ionic conductance (Fig 3A) as described previously (Anthony et al., 2000), which was reversible by 2 h incubation in saline without membrane-permeable cGMP (Kourghi et al., 2016). Re-activation of the ionic response by a second dose of cGMP was partly blocked in AQP1-expressing oocytes after 2 h incubation in 50 μ M bacopaside I, and strongly blocked at 100 μ M bacopaside I (Fig 3B). In contrast, the reactivation of the ion conductance was unimpaired after incubation with 10 μ M or 20 μ M bacopaside II.

Identification of candidate intracellular binding sites. Protein crystal structures of AQP1 and AQP4, and three-dimensional structural renditions of bacopaside I and bacopaside II were prepared and run on interaction simulations using Autodock Vina software to identify predicted binding sites. An array of candidate docking sites for bacopasides I and II on AQP1 and -4 channels were considered with in silico computational docking analyses. Of a total of 8 possible positions evaluated for bacopaside I, the dominant energetically-favored

configurations for intracellular binding yielded values of -9.2 Kcal/mol for AQP1 (Data Supplement 1), and -8.0 Kcal/mol for AQP4 (Data Supplement 2). Similarly out of all possible positions evaluated, the energetically-favored configurations for bacopaside II yielded values of -9.3 Kcal/mol for AQP1 (Data Supplement 3), and -7.8 Kcal/mol for AQP4 (Data Supplement 4).

In the poses reflecting the most favored docking positions, the intracellular face of the water pore was effectively occluded by bacopasides I and II in AQP1, but not in AQP4 channels (Fig 4A,B,C,D). For AQP1, the bacopasides appeared to nest well into the internal vestibule of the intrasubunit water pore. For AQP4 the optimal interaction was seen for bacopaside sitting in a groove between transmembrane domains 4 and 5, a position where subunits interface near the central pore that might not be accessible in the assembled tetrameric channel.

Closer inspection of specific amino acid residues in the predicted AQP1 docking site (using Chimera visualization software) suggested that the poly-arginine motif in the Loop D domain could enable hydrogen bond formation with the sulfonyl moiety on the glucopyranosyl sugar of bacopaside I (Fig 4E) at residues corresponding to R159 and R160 in human AQP1. These arginines are part of a highly conserved amino acid pattern seen in AQP1 channels from diverse species, and required for cGMP gating of the AQP1 ionic conductance (Yu et al., 2006). The site-directed double mutation of arginines R159 and R160 to alanines did not prevent normal expression of AQP1-mediated osmotic water permeability, indicating that the AQP1 mutant constructs were expressed and targeted to the oocyte plasma membrane as described previously (Yu et al., 2006); however, the efficacy of bacopaside I in inhibiting osmotic water permeability was abolished in the mutant construct at doses up to 100 μ M (Figure 1D, supporting the suggested role of the loop D arginine residues in stabilizing the docking of the bacopaside I ligand).

Bacopaside II was more effective than bacopaside I in blocking migration of AQP1-expressing colon cancer cells. HT29 cells have a higher endogenous level of AQP1 expression as compared with SW480 cells, as demonstrated by quantitative RT-PCR (Fig. 5A), western blot (Fig. 5B), and immunocytochemistry (Fig 5C) analyses.

Wound closure assays showed robust migration of HT29 cells in medium with vehicle (Fig 6A), resulting in little open area remaining at 24 h. In contrast, treatment with bacopaside II (Fig. 6B) substantially reduced the amount of wound closure. Dose-dependent block of cell migration measured by wound closure (Fig 6C) was observed for both bacopaside I and bacopaside II on HT29 cells. The calculated IC₅₀ value for bacopaside I was approximately 48 μ M and for bacopaside II was 14 μ M in HT29 cells. There was a small reduction of migration observed for SW480 cells treated with bacopasides I and II (Fig 6C), which was consistent with the relatively low expression of AQP1 channels in this cell line.

Time-lapse imaging demonstrated bacopasides I and II differentially decreased the rate of migration of AQP1-expressing HT29 colon cancer cells. Cultured HT29 cancer cells showed differences in rates of migration into the open wound areas in the vehicle, bacopaside I and bacopaside II treatment conditions (Fig 7A,B,C). Time lapse images showed the rates of cell migration were significantly impeded in 50 μ M bacopaside I and in 15 μ M bacopaside II (Fig 7B,C) as compared with vehicle-treated HT29 cells (Fig 7A). No appreciable difference in cell viability was observed in any of the treatment groups during the 24 time course of the experiment.

In the vehicle-treated group, trajectory plots of individual cells sampled at 50 min intervals over 24 h (Fig 7D) showed generally directional movements of HT29 cells into the open wound spaces. In bacopaside I treatment group, the HT29 cells lacked directional migration and moved short distances between successive frames. In the bacopaside II treated group, the impairment of movement was evident but less severe. The collective trend of trajectories of the vehicle-treated group appeared to be linear and extended, whereas that in the

bacopaside I treated group was recursive and compressed; the bacopaside II group showed an intermediate level of restriction of movement.

The net displacement (distance travelled) per time interval was greater in the vehicle-treated group than in the bacopasides I and II treatment groups. Frequency histograms, summarizing all events observed, were compiled as the binned values of distances travelled per 50 min interval (Fig 7E). These histograms showed that more cells travelled longer distances per time interval in the vehicle-treated group than in the bacopaside-treated groups. Distributions moved were well fit by Gaussian functions; the decreased mean distances moved in the bacopaside treatments were seen as left shifts in the peaks of the frequency histograms. Compiled data in a summary histogram (Fig 7F) confirmed the significant decrease in mean total distance travelled by cells during the 24 hours of tracking in bacopaside I or II as compared with vehicle-treated cells. Analysis of cytotoxicity by AlamarBlue assay showed that bacopaside I had no significant effect on cell viability at 50 or 75 μ M, and bacopaside II had no effect on viability at 15 or 20 μ M (Table 1). Concentrations of bacopasides that significantly blocked AQP1 water channel activity and HT29 cell migration were not appreciably cytotoxic.

Discussion

Results here demonstrated that two structurally similar compounds, bacopaside I and bacopaside II derived from a medicinal herb, act differentially as pharmacological inhibitors of mammalian aquaporin channels. In silico modeling predicted that bacopasides I and II have favorable energies of interaction at the intracellular vestibule of AQP1, occluding the intrasubunit water pore. Modeling results were consistent with observed effects of these agents as AQP1 inhibitors. Predicted energies of interaction for docking on AQP1 were higher for bacopaside II than bacopaside I, fitting the observed order of efficacy in blocking AQP1-mediated swelling of oocytes and the same order of efficacy in blocking migration of AQP1-expressing HT29 colon cancer cells, with minimal effects on SW480 cells that express little AQP1. The docking of bacopasides I and II to occlude the water pore appeared principally to involve the trisaccharide rings, which projected down into the AQP1 intrasubunit pore. Future work exploring polysaccharides and related osmolytes as endogenous modulators of AQP channels could be of interest. The lack of a favorable docking interaction of bacopaside with the AQP4 water pore was consistent with the insensitivity of AQP-4 expressing oocytes to bacopaside I in osmotic swelling assays. Based on the docking model, candidate residues that could contribute to the proposed binding of bacopaside sugar rings in the hAQP1 intracellular water pore appear to include amino acids serine 71 in the loop B region, and tyrosine 97 in the adjacent membrane spanning domains, but remain to be defined.

Inhibition of AQP1 water channel activity by bacopasides I and II showed a slow onset that was consistent with prerequisite transit of the agent across the membrane to access the intracellular side. The latency period (approximately 2 h) was comparable to that described for other aquaporin modulators AqB013 and AqF026, also thought to act at the cytoplasmic side (Migliati et al., 2009; Yool et al., 2013).

Accumulating evidence suggests pharmacological agents can be defined with subtype selectivity for AQP classes. Prior work showed external application of AqF026 potentiated water permeability in AQP1 (EC_{50} 3.3 μ M), but a 15-fold higher concentration was required to potentiate AQP4 (Yool et al., 2013). Metal complexes acted as blockers of glycerol permeability in AQP3 (at an external site predicted to involve cysteine (C40) and arginine (R218) residues), with comparatively small effects on AQP1 water permeability (Martins et al., 2013). Results here for bacopaside I showed block of osmotic water permeability for AQP1 but not AQP4 channels. This difference in bacopaside sensitivity between related aquaporins suggests that the inhibitory effects seen for AQP1 are exerted directly on the heterologously expressed channel, and not due to side effects on endogenous oocyte channels or transporters.

The reversibility of block indicated that functional properties and expression of the channels in plasma membrane were not impaired. Data here cannot rule out actions of bacopasides on other molecules not yet assessed; however, the lack of effect of bacopaside on migration in SW480 cells with low AQP1 expression suggests the mechanism of action is reasonably selective, and does not appreciably impact diverse signalling and transport processes needed for basic maintenance and non-AQP1 dependent motility. Cytotoxicity assays showed the viability of AQP1-expressing HT29 cancer cells was not affected by bacopasides I and II at doses that significantly blocked ion flux and cell migration.

Bacopasides I and II are triterpene glycosides, composed of a hydrophobic pentacyclic terpene backbone (estimated logP value approximately 9; enabling membrane permeability), and three linked polar sugar groups (arabinofuranosyl—glucopyranosyl—arabinopyranose in bacopaside I; and arabinofuranosyl—sulfonyl-glucopyranosyl—glucopyranose in bacopaside II) that appear from in silico modeling to lodge via H-bonds into the water pore entrance of AQP1, with the exception of the sulfonyl group which appears to require an interface with positively charged residues (arginines in the adjacent AQP1 Loop D domain). Mutation of the key Loop D arginines to alanines appeared to cause destabilization of the overall binding

of the bacopaside I compound on AQP1, seen as a decreased efficacy of water pore block and increased IC_{50} value in the R159A+R160A mutant.

The ability of modulators to block the central pore ionic conductance is an important consideration in processes such as rapid cell migration which appear to require the AQP1 cation channel activity (Kourghi et al., 2016). Interaction of the sulfonyl group with Loop D arginines was consistent with the observed block of the cGMP-activated ionic conductance by bacopaside I, not II. Bacopaside II lacked an effect on the ionic conductance, and showed similar IC_{50} values for the block of AQP1 water channel activity in oocytes, and the block of cell migration in HT29 cells. In contrast, bacopaside I showed a lower IC_{50} value for inhibiting HT29 cancer cell migration ($\sim 48 \mu M$) than for inhibiting the AQP1 osmotic water flux in oocytes ($\sim 117 \mu M$), suggesting that simultaneous block of both water and ion channel activities of AQP1 might be more effective in blocking cell migration. This is consistent with the observed migration trajectories, which were more compressed in bacopaside I-treated group than in the bacopaside II-treated group.

Although the overall amino acid sequence similarity between AQP1 and AQP4 channels is high (>40% identity and 60% homology), AQP4-mediated osmotic swelling was not sensitive to block by bacopaside I. The docking model suggested the bulky terpene might sterically hinder docking near the AQP4 water pore. As well, the Loop D domain of AQP4 lacks the key arginines 159 and 160 suggested here to be important for the sulfonyl group coordination, showing instead serine and lysine in the equivalent positions, which might be less effective as putative coordination sites.

The identification of bacopasides as novel AQP modulators expands the database of pharmacophore properties of AQP ligands. Bacopasides I and II themselves might not be ideal as drug candidates, exceeding limits of Lipinski's Rule of Five for molecular weight, hydrophobicity, and numbers of hydrogen bond donors and acceptors— although natural products often show biological activity as exceptions to the rule (Ganesan, 2008).

Bacopasides administered in vivo are likely to act as metabolic derivatives as well as intact compounds. More work is needed to define in vivo metabolites of bacopasides and characterize their effects on aquaporins. Nonetheless, bacopasides could serve as lead compounds for the design of small-molecule blockers of aquaporins. Results here suggest the trisaccharide moiety is a key component. An intriguing idea would be to design compact membrane-permeable trisaccharides for blocking water flux; addition of key sulfonyl or other groups could inhibit parallel AQP functions. Endogenous polysaccharide osmolytes in cells might function as natural modulators of aquaporin channels, a concept that has not to our knowledge been considered previously.

Bacopa monnieri extract (also known as brahmi) has been used in Ayurvedic remedies since ancient times to improve memory and treat anxiety and depression (Russo and Borrelli, 2005). Brahmi has been suggested to have beneficial effects on psychological state, cognitive performance, and memory in human subjects and animal models; neuroprotective effects after ischemic brain injury; and anti-inflammatory actions in processes linked to neurodegenerative disorders (Aguilar and Borowski, 2013; Downey et al., 2013; Kongkeaw et al., 2014; Liu et al., 2013; Rehni et al., 2007; Sairam et al., 2002; Saraf et al., 2010; Singh and Dhawan, 1982; Williams et al., 2014; Zhou et al., 2007). A meta-analysis of human clinical studies (generally with *B. monnieri* administered 250-450 mg/day for up to several months) improved mental response time and attention, and had potential benefits on memory (Kongkeaw et al., 2014). No serious adverse events were noted; minor side effects included diarrhea and dry mouth.

Beneficial outcomes ascribed to brahmi could in part involve block of AQP1 channels. AQP1 is expressed abundantly in brain choroid plexus where cerebral spinal fluid is produced (Boassa and Yool, 2005; Johansson et al., 2005), and in proximal kidney to facilitate water reabsorption (Nielsen and Agre, 1995). AQP1 is found in peripheral vasculature endothelia, red blood cells, and other cell types (Nielsen et al., 1993). Block of AQP1 could contribute to the anti-inflammatory benefits of brahmi treatment. Macrophages express AQP1 channels,

which are required for IL-1 β release and neutrophilic inflammation responses (Rabolli et al., 2014). An alcoholic extract of *B. monnieri* decreased TNF- α production in mouse macrophages preincubated for 1 h, with an IC₅₀ near 1 mg/ml (Williams et al., 2014).

Pharmacological inhibitors of AQP1 channels could be useful for intervention in many conditions, including slowing metastasis in AQP1-positive cancer subtypes. In a subset of aggressive cancers, AQP1 expression is upregulated (El Hindy et al., 2013; Moon et al., 2003; Saadoun et al., 2002; Yool et al., 2009). AQP1 channels located at lamellipodial edges have been implicated in enhancing migration and metastasis (Hu and Verkman, 2006; McCoy and Sontheimer, 2007). Block of the AQP1 ion channel impairs migration in AQP1-expressing HT29 colon cancer cells (Kourghi et al., 2016).

A comprehensive portfolio of selective aquaporin modulators is needed for clinical and basic research. Further exploration of AQP modulators in traditional herbal medicines is merited (Pei et al., 2016). New ligand modulators of aquaporin channel activity could be present in the armamentarium of traditional herbal medicines, but remain to be discovered.

Acknowledgments

Thanks to John Sandham and The Botanic Gardens of Adelaide for identified samples of the water hyssop *Bacopa monnieri*; and to Dr Agatha Labrinidis and the Adelaide Microscopy core facility for access to equipment, support and training in live cell imaging.

Authorship contributions

Participated in the research design: Pei, Campbell, Yool, Hardingham

Conducted experiments: Pei, Kourghi, De Ieso, Campbell, Doward

Performed data analysis: Pei, Kourghi, De Ieso, Yool

Wrote or contributed to writing of the manuscript: Pei, Kourghi, De Ieso, Yool

References

- Agre P, Preston GM, Smith BL, Jung JS, Raina S, Moon C, Guggino WB and Nielsen S (1993) Aquaporin CHIP: the archetypal molecular water channel. *The American journal of physiology* **265**(4 Pt 2):F463-476.
- Aguiar S and Borowski T (2013) Neuropharmacological review of the nootropic herb *Bacopa monnieri*. *Rejuvenation Res* **16**(4):313-326.
- Anthony TL, Brooks HL, Boassa D, Leonov S, Yanochko GM, Regan JW and Yool AJ (2000) Cloned human aquaporin-1 is a cyclic GMP-gated ion channel. *Mol Pharmacol* **57**(3):576-588.
- Boassa D and Yool AJ (2003) Single amino acids in the carboxyl terminal domain of aquaporin-1 contribute to cGMP-dependent ion channel activation. *BMC Physiol* **3**:12.
- Boassa D and Yool AJ (2005) Physiological roles of aquaporins in the choroid plexus. *Curr Top Dev Biol* **67**:181-206.
- Brooks HL, Regan JW and Yool AJ (2000) Inhibition of aquaporin-1 water permeability by tetraethylammonium: involvement of the loop E pore region. *Molecular pharmacology* **57**(5):1021-1026.
- Calamita G, Bishai WR, Preston GM, Guggino WB and Agre P (1995) Molecular cloning and characterization of AqpZ, a water channel from *Escherichia coli*. *The Journal of biological chemistry* **270**(49):29063-29066.
- Campbell EM, Birdsell DN and Yool AJ (2012) The activity of human aquaporin 1 as a cGMP-gated cation channel is regulated by tyrosine phosphorylation in the carboxyl-terminal domain. *Mol Pharmacol* **81**(1):97-105.
- Detmers FJ, de Groot BL, Muller EM, Hinton A, Konings IB, Sze M, Flitsch SL, Grubmuller H and Deen PM (2006) Quaternary ammonium compounds as water channel blockers. Specificity, potency, and site of action. *J Biol Chem* **281**(20):14207-14214.
- Devuyst O and Yool AJ (2010) Aquaporin-1: new developments and perspectives for peritoneal dialysis. *Perit Dial Int* **30**(2):135-141.
- Downey LA, Kean J, Nemeh F, Lau A, Poll A, Gregory R, Murray M, Rourke J, Patak B, Pase MP, Zangara A, Lomas J, Scholey A and Stough C (2013) An Acute, Double-Blind, Placebo-Controlled Crossover Study of 320 mg and 640 mg Doses of a Special

Extract of *Bacopa monnieri* (CDRI 08) on Sustained Cognitive Performance.

Phytother Res **27**:1407-1413.

El Hindy N, Bankfalvi A, Herring A, Adamzik M, Lambertz N, Zhu Y, Siffert W, Sure U and Sandalcioğlu IE (2013) Correlation of aquaporin-1 water channel protein expression with tumor angiogenesis in human astrocytoma. *Anticancer research* **33**(2):609-613.

Esteva-Font C, Jin BJ, Lee S, Phuan PW, Anderson MO and Verkman AS (2016) Experimental Evaluation of Proposed Small-Molecule Inhibitors of Water Channel Aquaporin-1. *Mol Pharmacol* **89**(6):686-693.

Fu D, Libson A, Miercke LJ, Weitzman C, Nollert P, Krucinski J and Stroud RM (2000) Structure of a glycerol-conducting channel and the basis for its selectivity. *Science* **290**(5491):481-486.

Ganesan A (2008) The impact of natural products upon modern drug discovery. *Curr Opin Chem Biol* **12**(3):306-317.

Gao J, Wang X, Chang Y, Zhang J, Song Q, Yu H and Li X (2006) Acetazolamide inhibits osmotic water permeability by interaction with aquaporin-1. *Analytical biochemistry* **350**(2):165-170.

Hu J and Verkman AS (2006) Increased migration and metastatic potential of tumor cells expressing aquaporin water channels. *FASEB journal : official publication of the Federation of American Societies for Experimental Biology* **20**(11):1892-1894.

Huber VJ, Tsujita M, Kwee IL and Nakada T (2009) Inhibition of aquaporin 4 by antiepileptic drugs. *Bioorg Med Chem* **17**(1):418-424.

Huber VJ, Tsujita M, Yamazaki M, Sakimura K and Nakada T (2007) Identification of arylsulfonamides as Aquaporin 4 inhibitors. *Bioorg Med Chem Lett* **17**(5):1270-1273.

Johansson PA, Dziegielewska KM, Ek CJ, Habgood MD, Møllgård K, Potter A, Schuliga M and Saunders NR (2005) Aquaporin-1 in the choroid plexuses of developing mammalian brain. *Cell Tissue Res* **322**(3):353-364.

Kongkeaw C, Dilokthornsakul P, Thanarangsarit P, Limpeanchob N and Norman Scholfield C (2014) Meta-analysis of randomized controlled trials on cognitive effects of *Bacopa monnieri* extract. *J Ethnopharmacol* **151**(1):528-535.

- Kourghi M, Pei JV, De Ieso ML, Flynn G and Yool AJ (2016) Bumetanide Derivatives AqB007 and AqB011 Selectively Block the Aquaporin-1 Ion Channel Conductance and Slow Cancer Cell Migration. *Mol Pharmacol* **89**(1):133-140.
- Liu X, Yue R, Zhang J, Shan L, Wang R and Zhang W (2013) Neuroprotective effects of bacopaside I in ischemic brain injury. *Restorative neurology and neuroscience* **31**(2):109-123.
- Martins AP, Ciancetta A, de Almeida A, Marrone A, Re N, Soveral G and Casini A (2013) Aquaporin inhibition by gold(III) compounds: new insights. *Chem Med Chem* **8**(7):1086-1092.
- McCoy E and Sontheimer H (2007) Expression and function of water channels (aquaporins) in migrating malignant astrocytes. *Glia* **55**(10):1034-1043.
- Migliati E, Meurice N, DuBois P, Fang JS, Somasekharan S, Beckett E, Flynn G and Yool AJ (2009) Inhibition of aquaporin-1 and aquaporin-4 water permeability by a derivative of the loop diuretic bumetanide acting at an internal pore-occluding binding site. *Mol Pharmacol* **76**(1):105-112.
- Moon C, Soria JC, Jang SJ, Lee J, Obaidul Hoque M, Sibony M, Trink B, Chang YS, Sidransky D and Mao L (2003) Involvement of aquaporins in colorectal carcinogenesis. *Oncogene* **22**(43):6699-6703.
- Nielsen S and Agre P (1995) The aquaporin family of water channels in kidney. *Kidney Int* **48**(4):1057-1068.
- Nielsen S, Smith BL, Christensen EI and Agre P (1993) Distribution of the aquaporin CHIP in secretory and resorptive epithelia and capillary endothelia. *Proc Natl Acad Sci U S A* **90**(15):7275-7279.
- Niemietz CM and Tyerman SD (2002) New potent inhibitors of aquaporins: silver and gold compounds inhibit aquaporins of plant and human origin. *FEBS letters* **531**(3):443-447.
- Papadopoulos MC and Verkman AS (2008) Potential utility of aquaporin modulators for therapy of brain disorders. *Prog Brain Res* **170**:589-601.
- Parsels LA, Parsels JD, Tai DC, Coughlin DJ and Maybaum J (2004) 5-fluoro-2'-deoxyuridine-induced cdc25A accumulation correlates with premature mitotic entry and clonogenic death in human colon cancer cells. *Cancer Res* **64**(18):6588-6594.

- Pei JV, Burton JL, Kourghi M, De Ieso ML and Yool AJ (2016) Drug discovery and therapeutic targets for pharmacological modulators of aquaporin channels., in *Aquaporins in Health and Disease: New Molecular Targets For Drug Discovery* (Soveral G, Casinin A and Nielsen S eds) pp 275-297., CRC Press, Oxfordshire, UK.
- Preston GM, Jung JS, Guggino WB and Agre P (1993) The mercury-sensitive residue at cysteine 189 in the CHIP28 water channel. *The Journal of biological chemistry* **268**(1):17-20.
- Rabolli V, Wallemme L, Lo Re S, Uwambayinema F, Palmari-Pallag M, Thomassen L, Tyteca D, Octave JN, Marbaix E, Lison D, Devuyst O and Huaux F (2014) Critical role of aquaporins in interleukin 1beta (IL-1beta)-induced inflammation. *J Biol Chem* **289**(20):13937-13947.
- Rehni AK, Pantlya HS, Shri R and Singh M (2007) Effect of chlorophyll and aqueous extracts of *Bacopa monniera* and *Valeriana wallichii* on ischaemia and reperfusion-induced cerebral injury in mice. *Indian journal of experimental biology* **45**(9):764-769.
- Reizer J, Reizer A and Saier MH, Jr. (1993) The MIP family of integral membrane channel proteins: sequence comparisons, evolutionary relationships, reconstructed pathway of evolution, and proposed functional differentiation of the two repeated halves of the proteins. *Critical reviews in biochemistry and molecular biology* **28**(3):235-257.
- Russo A and Borrelli F (2005) *Bacopa monniera*, a reputed nootropic plant: an overview. *Phytomedicine : international journal of phytotherapy and phytopharmacology* **12**(4):305-317.
- Saadoun S, Papadopoulos MC, Davies DC, Bell BA and Krishna S (2002) Increased aquaporin 1 water channel expression in human brain tumours. *British journal of cancer* **87**(6):621-623.
- Sairam K, Dorababu M, Goel RK and Bhattacharya SK (2002) Antidepressant activity of standardized extract of *Bacopa monniera* in experimental models of depression in rats. *Phytomedicine : international journal of phytotherapy and phytopharmacology* **9**(3):207-211.
- Saparov SM, Kozono D, Rothe U, Agre P and Pohl P (2001) Water and ion permeation of aquaporin-1 in planar lipid bilayers. Major differences in structural determinants and stoichiometry. *J Biol Chem* **276**(34):31515-31520.

- Saraf MK, Prabhakar S and Anand A (2010) Neuroprotective effect of *Bacopa monniera* on ischemia induced brain injury. *Pharmacology, biochemistry, and behavior* **97**(2):192-197.
- Schindelin J, Arganda-Carreras I, Frise E, Kaynig V, Longair M, Pietzsch T, Preibisch S, Rueden C, Saalfeld S, Schmid B, Tinevez JY, White DJ, Hartenstein V, Eliceiri K, Tomancak P and Cardona A (2012) Fiji: an open-source platform for biological-image analysis. *Nat Methods* **9**(7):676-682.
- Seeliger D, Zapater C, Krenc D, Haddoub R, Flitsch S, Beitz E, Cerda J and de Groot BL (2013) Discovery of novel human aquaporin-1 blockers. *ACS Chem Biol* **8**(1):249-256.
- Singh HK and Dhawan BN (1982) Effect of *Bacopa monniera* Linn. (brahmi) extract on avoidance responses in rat. *Journal of ethnopharmacology* **5**(2):205-214.
- Tajkhorshid E, Nollert P, Jensen MO, Miercke LJ, O'Connell J, Stroud RM and Schulten K (2002) Control of the selectivity of the aquaporin water channel family by global orientational tuning. *Science* **296**(5567):525-530.
- Trott O and Olson AJ (2010) AutoDock Vina: improving the speed and accuracy of docking with a new scoring function, efficient optimization, and multithreading. *Journal of computational chemistry* **31**(2):455-461.
- Williams R, Munch G, Gyengesi E and Bennett L (2014) *Bacopa monnieri* (L.) exerts anti-inflammatory effects on cells of the innate immune system in vitro. *Food Funct* **5**(3):517-520.
- Yang B, Kim JK and Verkman AS (2006) Comparative efficacy of HgCl₂ with candidate aquaporin-1 inhibitors DMSO, gold, TEA⁺ and acetazolamide. *FEBS Lett* **580**(28-29):6679-6684.
- Yool AJ (2007) Functional domains of aquaporin-1: keys to physiology, and targets for drug discovery. *Curr Pharm Des* **13**(31):3212-3221.
- Yool AJ, Brokl OH, Pannabecker TL, Dantzler WH and Stamer WD (2002) Tetraethylammonium block of water flux in Aquaporin-1 channels expressed in kidney thin limbs of Henle's loop and a kidney-derived cell line. *BMC physiology* **2**:4.
- Yool AJ, Brown EA and Flynn GA (2009) Roles for novel pharmacological blockers of aquaporins in the treatment of brain oedema and cancer. *Clin Exp Pharmacol Physiol* **37**(4):403-409.

- Yool AJ and Campbell EM (2012) Structure, function and translational relevance of aquaporin dual water and ion channels. *Mol Aspects Med* **33**(5):443-561.
- Yool AJ, Morelle J, Cnops Y, Verbavatz JM, Campbell EM, Beckett EA, Booker GW, Flynn G and Devuyst O (2013) AqF026 is a pharmacologic agonist of the water channel aquaporin-1. *Journal of the American Society of Nephrology : JASN* **24**(7):1045-1052.
- Yool AJ and Weinstein AM (2002) New roles for old holes: Ion channel function in aquaporin-1. *News Physiological Sciences* **17**:68-72.
- Yu J, Yool AJ, Schulten K and Tajkhorshid E (2006) Mechanism of gating and ion conductivity of a possible tetrameric pore in aquaporin-1. *Structure* **14**(9):1411-1423.
- Zhang W, Zitron E, Homme M, Kihm L, Morath C, Scherer D, Hegge S, Thomas D, Schmitt CP, Zeier M, Katus H, Karle C and Schwenger V (2007) Aquaporin-1 channel function is positively regulated by protein kinase C. *J Biol Chem* **282**(29):20933-20940.
- Zhou Y, Shen YH, Zhang C, Su J, Liu RH and Zhang WD (2007) Triterpene saponins from *Bacopa monnieri* and their antidepressant effects in two mice models. *Journal of natural products* **70**(4):652-655.

Footnotes

This work was supported by funding from the University of Adelaide Institute for Photonics and Advanced Sensing 2015 Pilot Grant program, and Australian Research Council Discovery Project grant DP160104641.

Legends for Figures

Figure 1. Block of osmotic water permeability in AQP1-expressing oocytes by water hyssop (*Bacopa monnieri*) extract, and constituent compounds bacopaside I and bacopaside II.

A. Mean swelling responses of AQP1-expressing oocytes in 50% hypotonic saline, standardized to the initial volume V_0 , were blocked by 2 h preincubation in reconstituted extract of water hyssop (at 1 mg/ml). Control non-AQP1 oocytes showed little change in volume. Data are mean values for all oocytes assessed from a single batch of oocytes; error bars are SEM; n values are 6 per treatment group. **B.** Column elution of methanol-extracted *Bacopa* identified two active fractions which caused block of AQP1 osmotic water permeability at 0.1 mg/ml each (which were further analyzed by mass spectroscopy to identify candidate compounds). Data are mean \pm SEM, n values in italics are above the x-axis. **C.** Candidate compounds bacopaside I and bacopaside II at 50 μ M differentially blocked osmotic water permeability in AQP1-expressing oocytes, causing a decrease in the rate of swelling as compared with untreated AQP1-expressing oocytes. Data are mean \pm SEM; n values are 8 (AQP1 vehicle), 5 (bacopaside I), 7 (bacopaside II), and 8 (non-AQP1 control). **D.** Dose-dependent block of AQP1-mediated osmotic swelling by bacopasides I and II, with estimated IC_{50} values of 117 μ M and 18 μ M, respectively. No sensitivity to bacopaside I was seen for the AQP1 R159,160A double mutant at doses up to 100 μ M. **E.** Chemical structures of bacopasides I and II.

Figure 2. Subtype selectivity and temporal properties of block onset and recovery with bacopasides I and II in AQP-expressing oocytes. **A.** Mean swelling responses of AQP4-expressing oocytes in 50% hypotonic saline were not affected after 2 h preincubation in 178 μ M bacopaside I. Data are mean \pm SEM; n values are 8 (AQP4 alone), 8 (AQP4 with bacopaside I), and 6 (non-AQP4 control). **B.** Time-dependent establishment of block of AQP1-mediated osmotic water permeability required preincubation of oocytes in 178 μ M bacopaside I or 35 μ M bacopaside II, with approximately 2 h needed to achieve maximal inhibition. n values are 12 to 14 oocytes per time point; each oocyte was used for a single measurement. **C.** Time-dependent recovery from block in AQP1-expressing oocytes preincubated 2 h in 178 μ M bacopaside I or 35 μ M bacopaside II, and assessed at different intervals after transfer back into standard isotonic saline at time 0 ('washout').

n values are 10 to 13 oocytes per time point; each oocyte was used for a single measurement.

Figure 3. Block of the cGMP-dependent ionic conductance of AQP1-expressing oocytes by bacopaside I, but not bacopaside II. **A.** Representative sets of traces recorded by two-electrode voltage clamp of AQP1-expressing oocytes showing the initial conductance; the response induced by the first application of membrane-permeable cGMP; the recovery of the response to near initial levels after 2 h incubation in isotonic saline containing bacopaside I (50 or 100 μ M) or bacopaside II (10 or 20 μ M); and the final response to a second application of cGMP. **B.** Trend plots showing the amplitude of the ionic currents, before and after the first activation by GMP, the recovery after incubation, and the response reactivated by a second cGMP application. Consistent recovery was seen after 10 or 20 μ M bacopaside II, but not after incubation with 50 or 100 μ M bacopaside I indicating establishment of ion channel block. n values are as shown; each line represents a series of recordings from one oocyte.

Figure 4. In silico docking models illustrating predictions for the most favorable sites of interaction of bacopaside I and bacopaside II on AQP1 and AQP4 subunit proteins. AQP subunit models were assembled from crystal structural data for human AQP1 (PDB ID. 1FQY) and human AQP4 (PDB ID. 3GDB); see Methods for details. Subunit views are from the cytoplasmic side, with the water pore in the center. The intracellular Loop D domain, adjacent to the channel tetrameric axis of symmetry, is highlighted in dark gold. **A.** Bacopaside I is predicted by in silico docking to occlude the cytoplasmic side of the intrasubunit water pore in AQP1. **B.** Favorable interactions at the AQP4 water pore are not evident for bacopaside I; the best fit is seen near membrane-spanning domains distant from the pore (inset). **C.** Bacopaside II is predicted to have the most favorable energy of interaction at a position occluding the cytoplasmic side of the AQP1 water pore. **D.** Predicted binding of bacopaside II with AQP4 is distant from the water pore (inset), in a position similar to that seen for bacopaside I. **E.** Enlarged view of the predicted

interaction of the sugar-linked sulfur group of bacopaside I with the conserved Loop D arginine residues in AQP1. **F.** Enlarged view of the predicted binding of the trisaccharide moiety of bacopaside II deep into the cytoplasmic vestibule of the AQP1 water pore.

Figure 5. HT29 cells have higher level of AQP1 expression than SW480 cells. **A.** The AQP1 RNA level was higher in HT29 cells as compared to SW480 cells as assessed using quantitative RT-PCR. **B.** The AQP1 protein level was higher in HT29 than SW480 cells as demonstrated by western blot, with monomeric subunit band seen near the predicted size of 28 kD with higher molecular weight glycosylated bands. **C.** The AQP1 immuno-positive signal (green) associated with the cell membrane was stronger in HT29 than in SW480 cells. Cell nuclei were counterstained (blue). See Methods for details.

Figure 6. Dose-dependent inhibition of migration by bacopasides I and II in AQP1-expressing HT29 cells, but not in SW480 cells with low AQP1 expression. Cell migration in the presence of a mitotic inhibitor was assessed by rates of closure of circular wounds, created by aspiration with a pipette tip in confluent cultures (see Methods for details). **A, B.** Cell migration was assessed in vehicle (A) or with 15 μ M bacopaside II (B) added immediately after wounding. Images are shown for confluent HT29 cultures after initial wounding at time 0 (upper panels) and at 24 h (lower panels). **C.** Dose-dependent block of HT29 cell migration was seen with bacopasides I and II, with IC₅₀ values estimated at 48 and 14 μ M respectively. Partial block of SW480 migration at the highest doses tested did not exceed 20%. Doses beyond the ranges shown were not considered valid due to the onset of cytotoxicity.

Figure 7. Live-cell imaging of the inhibitory effects of bacopasides I and II on migration of HT29 cells. Single cells at the boundaries of circular wounds were tracked with time-lapse images taken at 25 minute intervals for 10 hours at 37°C. **A, B, C.** Panels of six images each from time-lapse series are shown at 50 minute intervals: (A) HT29 cells with vehicle

treatment; **(B)** HT29 cells treated with 50 μ M bacopaside I; and **(C)** HT29 cells treated with 15 μ M bacopaside II. **D.** Trajectory plots of 10 individual cells per treatment group, monitored by cell nucleus position as a function of time. Data were converted to absolute values and referenced to the starting position at time 0; X and Y values are in pixels (7.45 pixels per mm). Trajectory plots illustrate the total movement of 10 individual cells per treatment over a duration of 600 min, with vehicle, bacopaside I or with bacopaside II. **E.** Frequency histograms of the distances moved by individual cells per 50 minute interval over 600 min of imaging, for 10 cells per treatment group. Histograms were fit with Gaussian distribution functions (R^2 values >0.94); best-fit values for the mean distances moved per cell per 50 min interval were 10.1 ± 0.5 for untreated, 4.7 ± 0.2 for bacopaside I treated and 7.8 ± 0.2 for bacopaside II treated (mean \pm SEM). **F.** Summary histogram showing the mean total distance travelled by cells in 600 min, showing significant inhibition of cell motility by both bacopaside I and II as compared to vehicle-treated cells (ANOVA test $p < 0.05$; posthoc Bonferroni $p < 0.05$ *, $p < 0.001$ ***). Data are mean \pm SEM; n values are 10 cells per treatment group.

Data supplement 1

pdb file showing the most favored docking position of bacopaside I on AQP1

Data supplement 2

pdb file showing the most favored docking position of bacopaside I on AQP4

Data supplement 3

pdb file showing the most favored docking position of bacopaside II on AQP1

Data supplement 4

pdb file showing the most favored docking position of bacopaside II on AQP4

Table 1. Analysis of cytotoxicity in HT29 colon cancer cells at 24 h treatment, using an AlumarBlue fluorescence assay.

Concentration (μ M)	Mean normalized cell viability (%), mean \pm SEM [§]	n value	signif
bacopaside I			
0	108 \pm 4.8	17	NS
0 (vehicle)	100 \pm 3.1	17	---
50	97 \pm 2.1	8	NS
75	79 \pm 4.2	8	NS
100	59 \pm 3.2	8	*
bacopaside II			
0	113 \pm 6.2	16	NS
0 (vehicle)	100 \pm 5.7	16	---
15	104 \pm 18	8	NS
20	123 \pm 17	8	NS
30	47 \pm 5.7	8	*
HgCl₂			
100	16.1 \pm 4.6	6	*

[§] Percent viability was standardized as a percentage of the vehicle-treated mean value, measured as changes in AlumarBlue fluorescence signal intensity. See Methods for details.

* Statistically significant differences ($p < 0.05$), compared with vehicle-treated, were analyzed by ANOVA with post-hoc Dunnett's multiple comparison test (GraphPad Prism). NS is not significant.

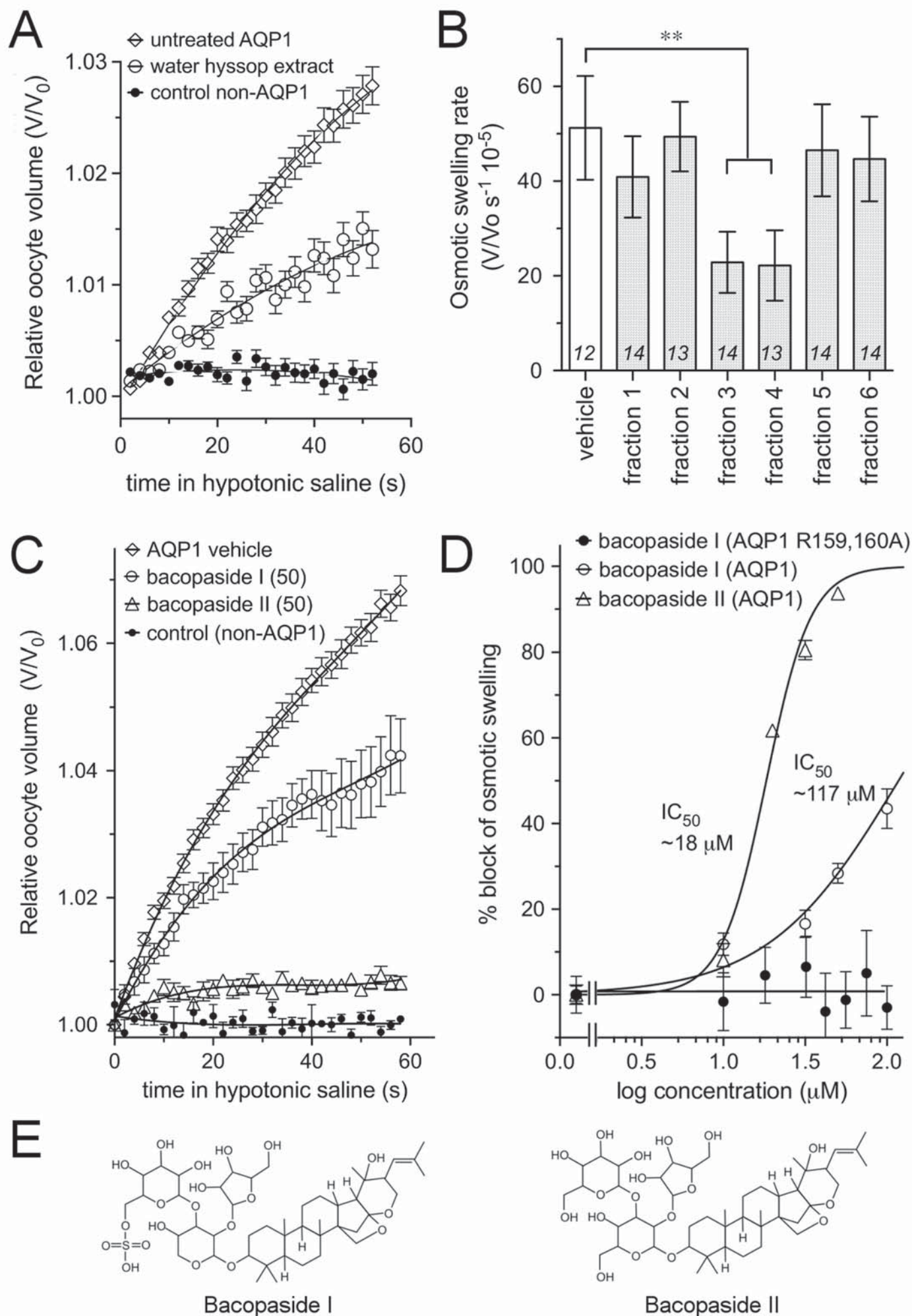


FIGURE 2

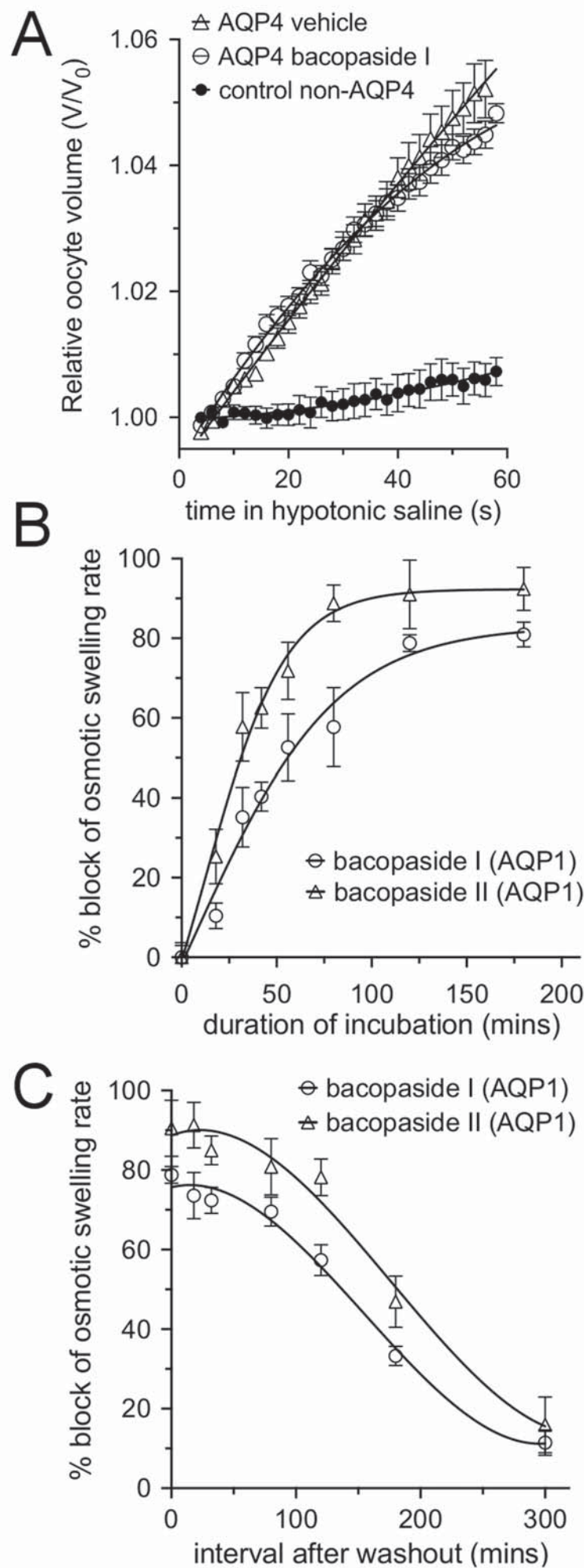


FIGURE 3

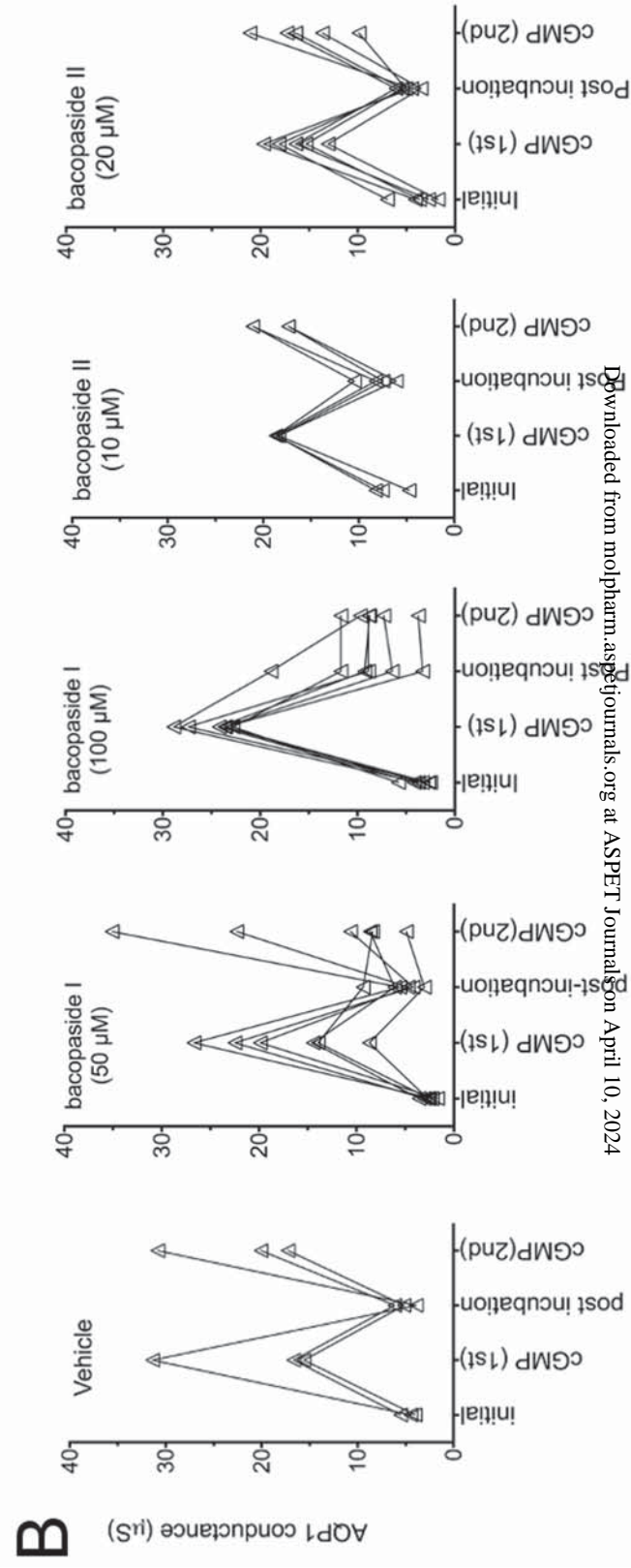
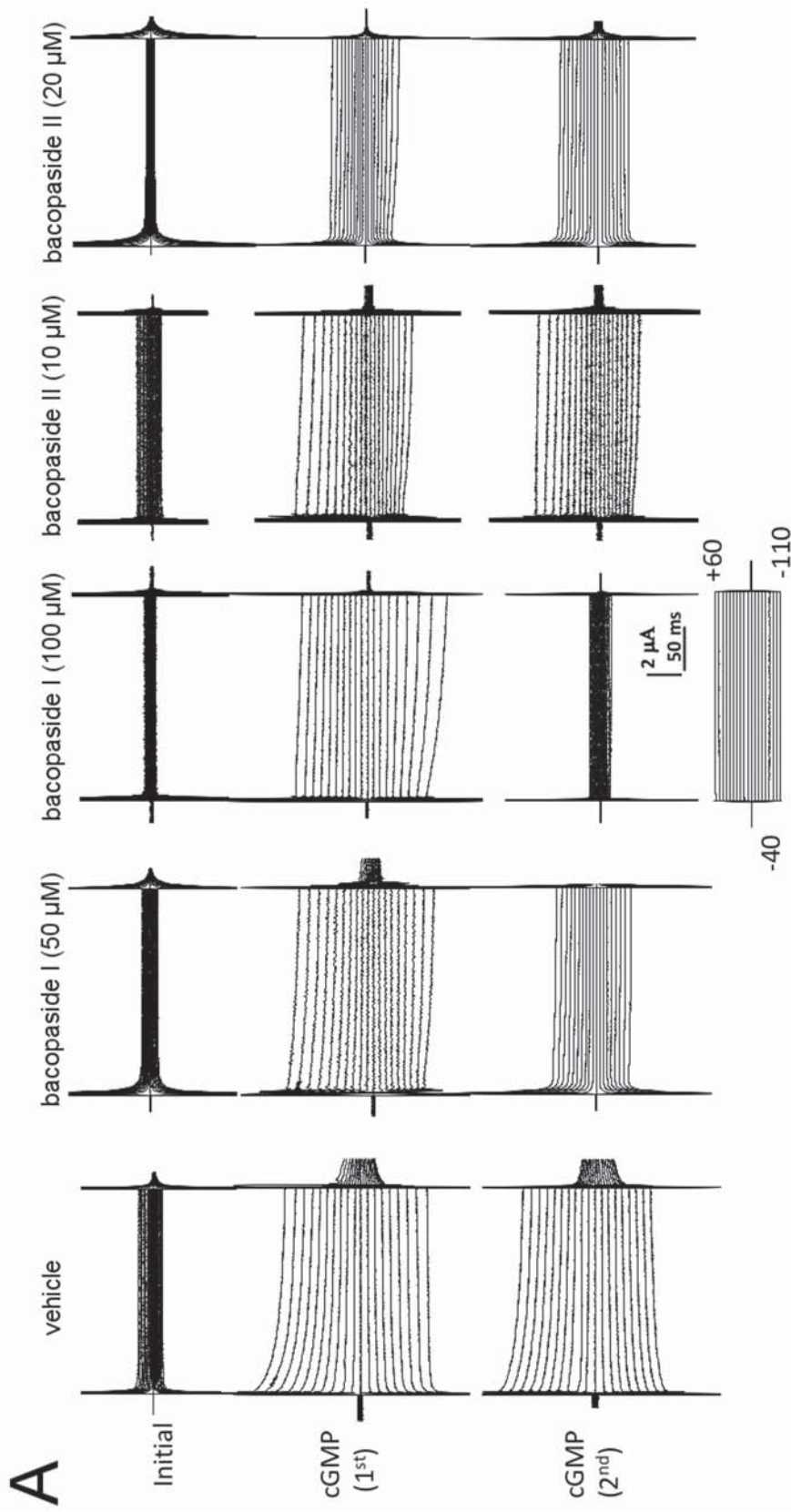


FIGURE 4

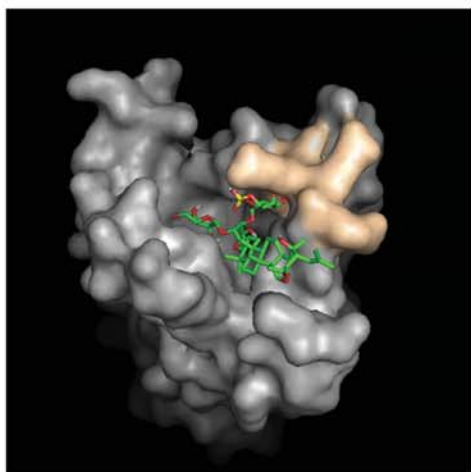
AQP1

AQP4

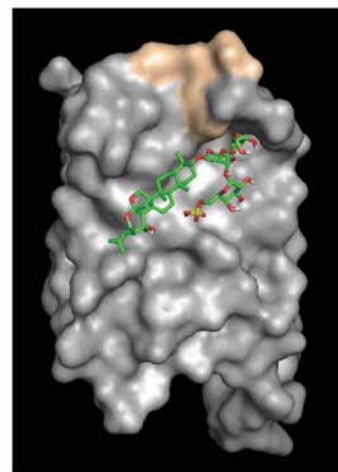
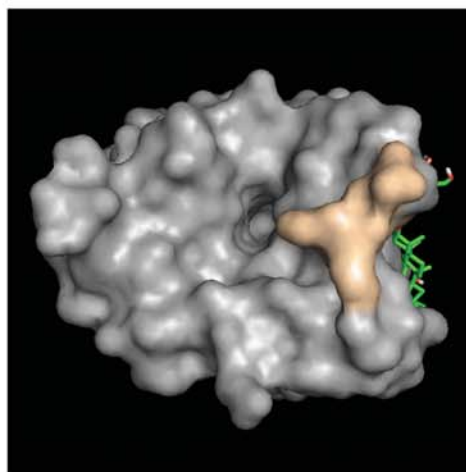
Downloaded from molpharm.aspetjournals.org at ASPET Journals on April 10, 2024

I
bacopaside
II
bacopaside

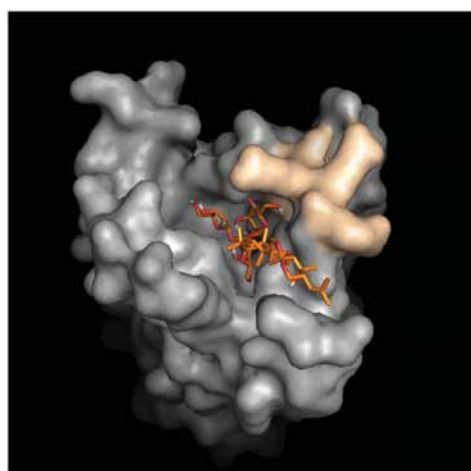
A



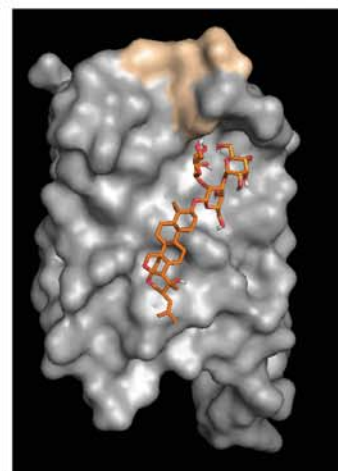
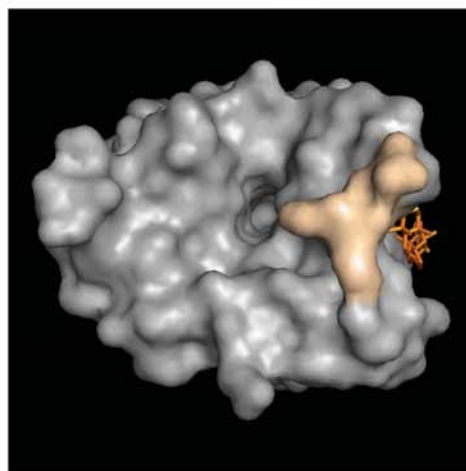
B



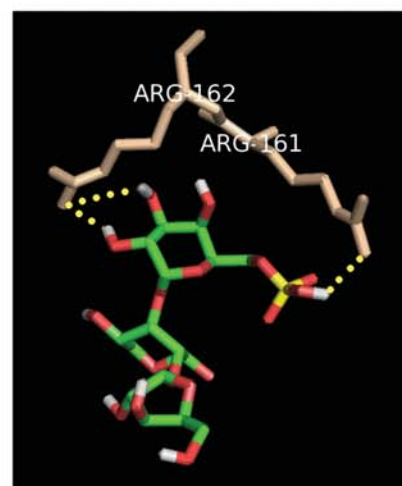
C



D



E



F

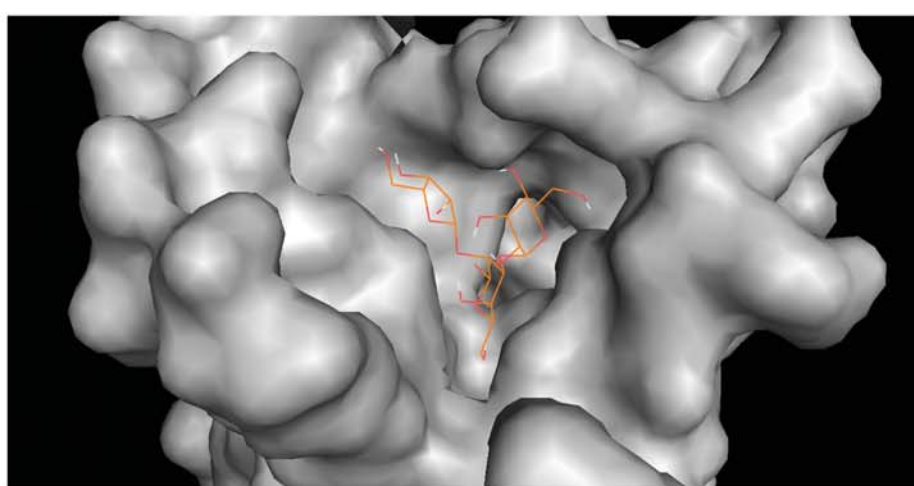


FIGURE 5

